

Turbulent Flow between Concentric Rotating Cylinders at Large Reynolds Number

Daniel P. Lathrop, Jay Fineberg, and Harry L. Swinney

Center for Nonlinear Dynamics and Department of Physics, University of Texas, Austin, Texas 78712
(Received 13 September 1991)

Turbulent Taylor vortex flow is studied in experiments for Reynolds numbers $10^3 < R < 10^6$. Simple scaling of the torque with Reynolds number is *not* observed for any range of R , although the characteristic time scales and the transport of passive scalars are found to scale with the global torque measurements. Above a nonhysteretic transition observed at $R = 1.3 \times 10^4$, the torque has a Reynolds number dependence similar to the drag observed in wall-bounded shear flows such as pipe flow and flow over a flat plate.

PACS numbers: 47.25.Ae, 47.20.Ft, 47.25.Ei, 47.25.Jn

Understanding the complexity of turbulence has long been a challenge to physicists [1]. As a system is driven to higher and higher values of the Reynolds number R , one might expect the details of the forcing to lose significance and universal behavior to emerge. Specifically, for high enough values of the Reynolds number, the global properties of the system could be expected to scale with R to some power. Such scaling was found in previous measurements of torque for flow between concentric rotating cylinders (Couette-Taylor flow) [2] and in experiments on convection-driven turbulence at high Rayleigh numbers [3].

The present experiments were undertaken to measure the scaling exponent α of the torque, $G \sim R^\alpha$, in Couette-Taylor turbulence for R up to 1.2×10^6 , which is far beyond the onset of Taylor vortices ($R_c = 82.4$) and the onset of chaos in this system ($R \sim 10^3$) [4]. Surprisingly, we have found no range in R in which the torque for turbulent flow exhibits a simple scaling with $\alpha = \text{const}$.

The scaling exponent for $R \rightarrow 0$ has been known since the work of Couette [5]: $\alpha = 1$. This result is the basis for Couette viscometry. In the opposite limit, $R \rightarrow \infty$, a prediction for α can be obtained from the Kolmogorov theory of turbulence [6]. The theory assumes that the dissipation rate ϵ per unit mass is a constant, independent of length scale for a wide range (the inertial range): $\epsilon = (\Delta U)^3/l$ for a velocity difference ΔU across a length l . We estimate ϵ using the largest length scale, $l = b - a$, where a and b are the radii of the inner and outer cylinders, and the corresponding velocity, $\Delta U = \Omega a$, where Ω is the rotation rate of the inner cylinder (the outer cylinder is at rest). Thus the torque, which is the total power dissipated ($\epsilon \times \text{volume}$) divided by the rotation rate, is given by $G = \pi[\eta(1 + \eta)/(1 - \eta)^2]R^2$, where $R = \Omega a(b - a)/\nu$, ν is the kinematic viscosity, ρ is the density, $\eta \equiv a/b$, and G is the dimensionless torque per unit length [7]. Thus $\alpha = 2$ for Kolmogorov turbulence.

An intermediate scaling regime might be expected in which there would be a turbulent core region with well-mixed angular momentum, and this core would be bounded by thin boundary layers near the inner and outer cylinder walls. This picture is supported by measurements of Smith and Townsend [8] in the range $7.3 \times 10^3 < R < 1.2 \times 10^5$. Marcus [9] showed that if the an-

gular momentum is assumed to be well mixed and the boundary layers are assumed to be at the critical Reynolds number for the onset of Taylor instability, then $G \sim R^{5/3}$.

We now describe our experiments and then we will compare our results with the predicted scaling exponents for turbulent flow, $\alpha = \frac{5}{3}$ and 2, and with results from other experiments.

Our apparatus consists of a stainless-steel inner cylinder of radius 16.00 cm and a transparent polished Plexiglas outer cylinder of radius 22.06 cm; thus $\eta = 0.7253$. The working section length L is 69.50 cm, giving an aspect ratio $\Gamma = L/(b - a) = 11.47$. To minimize end effects the inner cylinder is made in three sections with only the center one (43.2 cm long) sensing the torque; the center section is mounted on a set of low-friction bearings to decouple it from the end sections. The maximum rotation rate of the inner cylinder (16.5 Hz in water at 30°C) is set by the 2-kW power available from the motor. Heat is removed with cooling water pumped through the end plates, and the temperature is controlled to 0.1°C. Temperature measurements at several axial positions show that, even at the largest R , the fluid temperature is uniform to within 0.01°C.

The torque is determined from the deflection of a force-sensing arm that couples the center section of the inner cylinder to the shaft (this section would otherwise rotate freely). The deflection of the arm is measured with resistance strain gauges mounted on both sides of the arm; the gauges form two sides of an ac bridge whose output is measured with a lock-in detector. The torque measurements are calibrated by hanging weights at a known radius while the cylinder is held horizontally. A precision of 0.1% is achieved at all Reynolds numbers by using water-glycerol mixtures with different viscosities: 0.0080, 0.027, 0.070, 0.180, and 0.39 cm²/s at 30°C, as measured with Cannon-Fenske viscometers.

The wall shear stress is measured with a hot film probe (TSI model 1268W) mounted flush with the outer cylinder midway between the ends. The probe is calibrated using the torque measurements [10].

Flow patterns are visualized using a 0.1% concentration of Kalliroscope [11]. Photographs of the flow such as those in Fig. 1 show that the size of the smallest fluc-

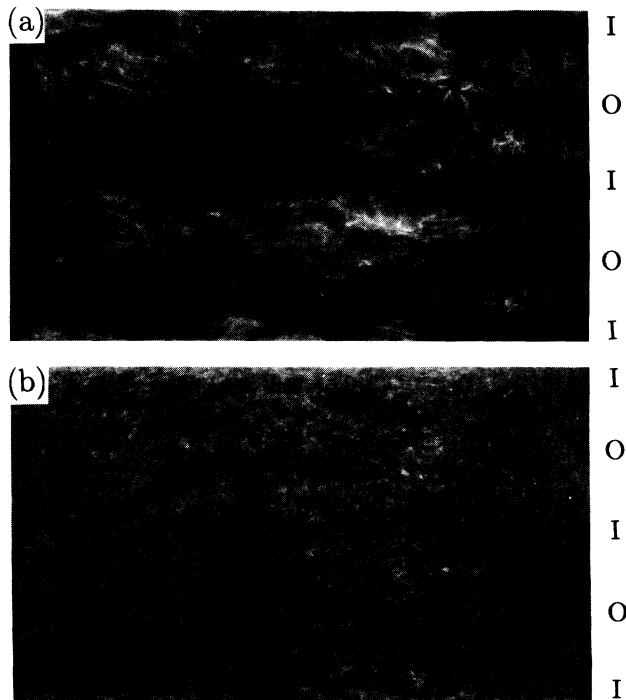


FIG. 1. Photographs of turbulent Taylor vortex flow at (a) $R=4600$ and (b) $R=15300$. (Taylor vortices first form at $R_c=82.4$.) The four vortices shown are from an eight-vortex state, corresponding to an average axial wavelength of $2.87(b-a)$. The letters indicate the inflow (*I*) and outflow (*O*) boundaries.

tuations decreases rapidly with increasing R , and the visibility of the Taylor vortices gradually decreases until they are no longer discernible for $R > 10^5$.

The torque measurements are shown in Fig. 2(a). The measurements were made with widely overlapping Reynolds number ranges for the five fluids. Analysis of these data, as we shall describe, reveals a previously unobserved transition at $R_T=1.3 \times 10^4$: For $R < R_T$ the data can be fitted with $G \sim R^\alpha$ with $\alpha=1.30$, while for $R > R_T$, $\alpha=1.73$ [12]. However, both below and above R_T the data clearly exhibit systematic deviations from simple power laws; hence we were led to examine the data more closely.

The high precision of our torque data enables us to determine the local exponent α from the slope of the graph of $\log G$ vs $\log R$ determined over a narrow range in R , $\Delta(\log_{10} R)=0.1$. To eliminate errors arising from the 0.5% uncertainty in the viscosity values, the exponent α is determined *separately* for each fluid. Figure 2(b) shows the result for α obtained by averaging (at each R) the values determined separately for each fluid. The conclusion is that there is *no* range in R for which the torque is described by a fixed exponent α . Rather, α increases monotonically from 1.23 at $R=2800$ to 1.87 at $R=1.2 \times 10^6$. The transition at $R_T=1.3 \times 10^4$ is apparent in Fig. 2(b): At R_T , $\partial\alpha/\partial(\log R)$ decreases by a factor of

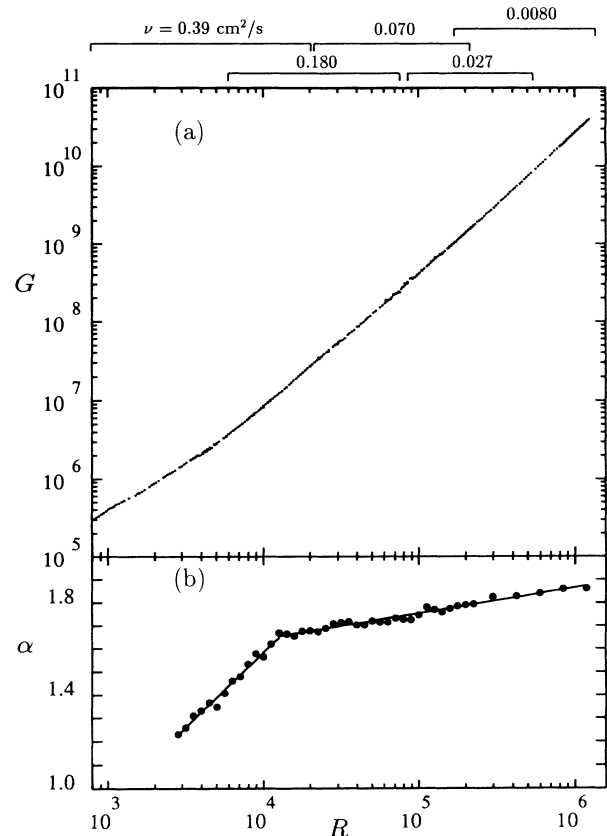


FIG. 2. (a) The measured nondimensionalized torque for the eight-vortex state [7]; (b) the corresponding local scaling exponent α . The straight lines in (b), which are drawn to guide the eye, are given by, for $R < R_T$, $\alpha=1.66+0.647 \log_{10}(R/R_T)$, and for $R > R_T$, $\alpha=1.66+0.111 \log_{10}(R/R_T)$; $R_T=1.3 \times 10^4$. The horizontal bars above the graph indicate the Reynolds number range for each fluid studied.

6 [2].

The value of the local α at transition is the same as that predicted by the marginal stability argument mentioned earlier, that is, $\alpha = \frac{5}{3}$. However, there is no regime where the marginal stability scaling holds; the local exponent simply passes through the marginal stability value. This contrasts with Rayleigh-Bénard convection, where the scaling of Nusselt number with Rayleigh number measured by Heslot, Castaing, and Libchaber and others is in reasonable accord with the marginal stability prediction, $Nu \sim Ra^{1/3}$, in the range $5 \times 10^5 < Ra < 4 \times 10^7$, beyond which there is a transition from “soft” to “hard” turbulence [3].

Our torque measurements together with earlier measurements by Tam and Swinney [13] of diffusion of dye in a turbulent Taylor vortex flow provide a direct test of the hypothesis that transport coefficients for momentum and for passive scalars should have the same scaling behavior [14]. This untested hypothesis is often made in analyses of turbulence and is crucial for understanding the interior structure of stars [15]. Our measurements

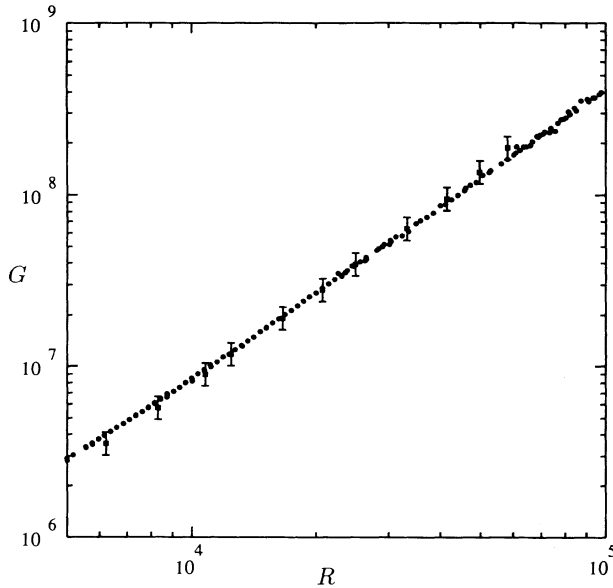


FIG. 3. A comparison of the torque computed from measurements of the axial diffusion coefficient (■) with the directly measured torque (●).

support this hypothesis, as we will now show.

Tam and Swinney injected pulses of dye into turbulent Taylor vortex flow and measured an effective axial diffusion coefficient D_{eff} [13]. Their results can be used to predict the torque (the radial transport of momentum), assuming that the effective diffusion coefficient for momentum ν_T is proportional to the dye diffusion coefficient, $\nu_T = cD_{\text{eff}}$, where c is an unknown prefactor. Hence the angular momentum flux across the gap between the cylinders is given by $J = cD_{\text{eff}}[\rho a^2 \Omega / (b-a)]$, where the term in brackets is the momentum gradient across the gap. The torque is given by the angular momentum flux times the area of the inner cylinder, $G = JA / \rho \nu^2 L = 2\pi \eta^2 c D_{\text{eff}} R / (1-\eta)^2 \nu$, where, as before, we have divided by $\rho \nu^2 L$ to make the torque dimensionless. The torque values predicted from the dye measurements (using $c = 0.176$) agree well with the direct measurements of torque, as Fig. 3 illustrates. The dye measurements did not have sufficient precision to reveal the transition at R_T that was found in the torque measurements. However, it was noted [13] that the local exponent for the scaling of the diffusion coefficient with R increased with increasing R , just as we find for the torque.

With increasing Reynolds number there is a decrease in the characteristic times for turbulent flow. We have obtained a time scale from a *local* measurement, the mean time between zero crossings of the wall shear stress [16], and a time scale from the *global* torque measurements; the latter time is given by the ratio of the shear velocity to the boundary layer thickness [17]. Remarkably, these two quantities exhibit the same scaling behavior, including strong curvature in the range 3.2×10^3

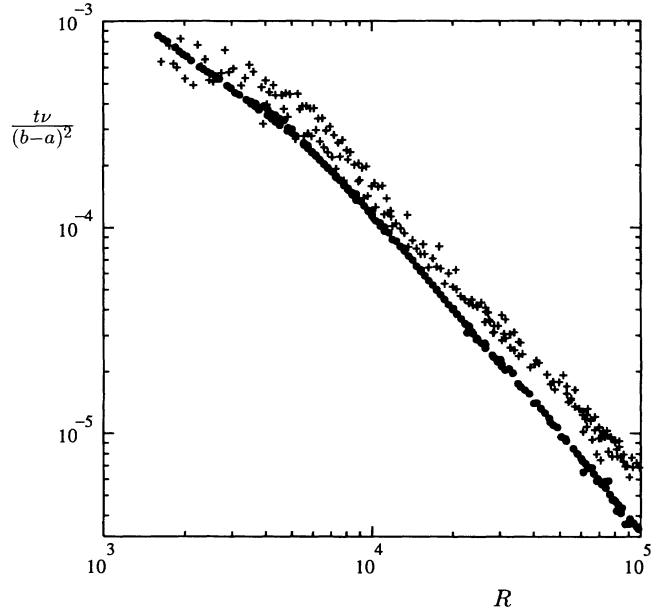


FIG. 4. The nondimensionalized time scales $\nu / (b-a)^2$ obtained from the zero crossings of the wall shear stress fluctuations, $\tau'_w = \tau_w - \langle \tau_w \rangle$, shown as (+), compared with times calculated from the torque measurements (●) [17].

$< R < 10^4$, as Fig. 4 illustrates.

The observed behavior of the torque at large R is consistent with previous observations of the turbulent drag in wall-bounded shear flows such as pipe flow and flow over a flat plate. Studies of such flows generally consider the skin friction coefficient, $c_f = F / (\frac{1}{2} \rho U_m^2 A)$, where F is the drag force, U_m a maximal velocity, and A a characteristic area. Wall-bounded shear flows have a mean velocity that varies logarithmically with the distance from the wall, except for a viscous sublayer very near the wall [18]. Assuming a logarithmic velocity profile in the boundary layers for the turbulent Taylor vortex flow, and matching the mean velocities at midgap, we obtain an equation governing the skin friction that is analogous to the Prandtl-von Kármán law for pipe flow [18], $c_f^{-1/2} = A \log R c_f^{1/2} + B$. Then, defining $c_f = G / R^2$, we have $R / \sqrt{G} = A \log \sqrt{G} + B$, which fits our data well (with $A = 1.52$ and $B = -1.63$ from a linear regression), as Fig. 5(a) demonstrates.

The good fit of our data by a Prandtl-von Kármán-type equation leads us to make a direct comparison of the skin friction for turbulent Taylor vortex flow with that determined for pipe flow and flow over a flat plate [Fig. 5(b)]. The similarity of the Reynolds number dependence of these skin friction coefficients points to similar fluid dynamics in all three cases, even though *a priori* one might expect to have major differences between the *closed* Couette-Taylor system, where the transition to a fully turbulent flow at R_T is nonhysteretic, and the *open* wall-bounded shear flows such as pipe flow and

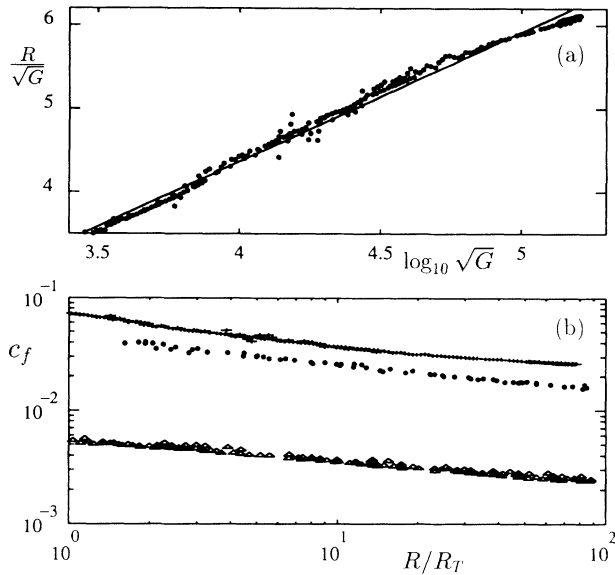


FIG. 5. (a) A fit of the torque data by a Prandtl-von Kármán-type law. (b) Skin friction coefficients for turbulent flows for the Couette-Taylor system (+), a pipe (●), and a flat plate (Δ), as a function of R/R_T , where R_T is taken to be the transition Reynolds number in the presence of background disturbances ($R_T = 1.3 \times 10^4$ for Taylor vortex flow, 2.3×10^3 for pipe flow [18], and 3.2×10^5 for a flat plate [18]).

flow over a plate, where the transition to turbulence exhibits large hysteresis. The local slope, which is $\alpha - 2$, increases in each case continuously with R , with α never exceeding $\alpha = 1.87$. This suggests that there may be a single fluid-dynamical description of turbulent wall-bounded shear flows, although some differences can be expected because of wall curvature and downstream pressure gradient effects.

Our early expectation was that the torque data would be described by one or more power laws. Each power law would cover its own range, and each could be explained by a different type of physics dominating the behavior in the boundary layer. What became apparent with successively more accurate torque measurements was that no single power law describes the behavior over any range of the data. At the highest Reynolds numbers, our largest observed exponent, $\alpha = 1.87$, is still well below the Kolmogorov limit, $\alpha = 2$. The starting assumption of the Kolmogorov estimate is equivalent to a statement about typical eddies in a turbulent flow: $\Delta U = \epsilon^{1/3} l^{1/3}$. Thus the theory predicts cube-root singularities in the flow field. We have

established a connection between this statement and the scaling of the torque $G \sim R^2$. Deviations from this prediction suggest that typical eddies follow a different scaling law also: $\Delta U \sim l^{(3-a)/(a+1)}$

We would like to thank R. Behringer, M. Crawford, P. S. Marcus, E. Siggia, E. Spiegel, and J. Weldon. This work is supported by ONR Grant No. N00014-89-J-1495.

- [1] U. Frisch and S. A. Orszag, *Phys. Today* **43**, No. 1, 24 (1990).
- [2] F. Wendt, *Ing. Arch.* **4**, 577 (1933).
- [3] F. Heslot, B. Castaing, and A. Libchaber, *Phys. Rev. A* **36**, 5870 (1987), and references therein.
- [4] A. Brandstater and H. L. Swinney, *Phys. Rev. A* **35**, 2207 (1987).
- [5] M. M. Couette, *Ann. Chim. Phys. Ser. VI* **21**, 433 (1890).
- [6] A. N. Kolmogorov, *C. R. Acad. Sci. URSS* **30**, 301 (1941).
- [7] The dimensionalized torque can be obtained by multiplying G by $\rho v^2 L$, where L is the length of the annulus.
- [8] G. P. Smith and A. A. Townsend, *J. Fluid Mech.* **123**, 187 (1982).
- [9] P. S. Marcus, *J. Fluid Mech.* **146**, 65 (1984); G. P. King, Y. Li, W. Lee, H. L. Swinney, and P. S. Marcus, *J. Fluid Mech.* **141**, 365 (1984); see also A. Barcion and J. Brindley, *J. Fluid Mech.* **143**, 429 (1984).
- [10] R. J. Goldstein, *Fluid Mechanics Measurements* (Hemisphere, Washington, DC, 1983).
- [11] P. Matisse and M. Gorman, *Phys. Fluids* **27**, 759 (1984).
- [12] Although not discussed at the time, the existence of the transition can be discerned from the torque measurements of Wendt [2] for all three radius ratios studied, 0.680, 0.850, and 0.935.
- [13] W. Y. Tam and H. L. Swinney, *Phys. Rev. A* **36**, 1374 (1987).
- [14] W. M. Kays and M. E. Crawford, *Convective Heat and Mass Transfer* (McGraw-Hill, New York, 1980), p. 207.
- [15] B. Chaboyer and J. P. Zahn, *Astron. Astrophys.* **253**, 173 (1992).
- [16] K. R. Sreenivasan, A. Prabhu, and R. Narasimha, *J. Fluid Mech.* **137**, 251 (1983).
- [17] The boundary layer time is given by $t_b \equiv u^*/\delta$, where $u^* \equiv (\tau_w/\rho)^{1/2} = (Gv^2/2\pi b^2)^{1/2}$. The thickness δ of the boundary layers at the cylinder walls can be estimated as follows: The wall shear stress is $\tau_w = \rho v |\partial U/\partial r|_{r=b} = G\rho v^2/2\pi b^2 = \rho v(\gamma\Omega a^2/b\delta)$, where γ is a constant taken to be 0.5, as suggested by the data of Smith and Townsend [8]. Thus $\delta = \pi a^2 b \Omega / Gv$.
- [18] H. Schlichting, *Boundary-Layer Theory* (McGraw-Hill, New York, 1979), 7th ed., pp. 598 and 639.

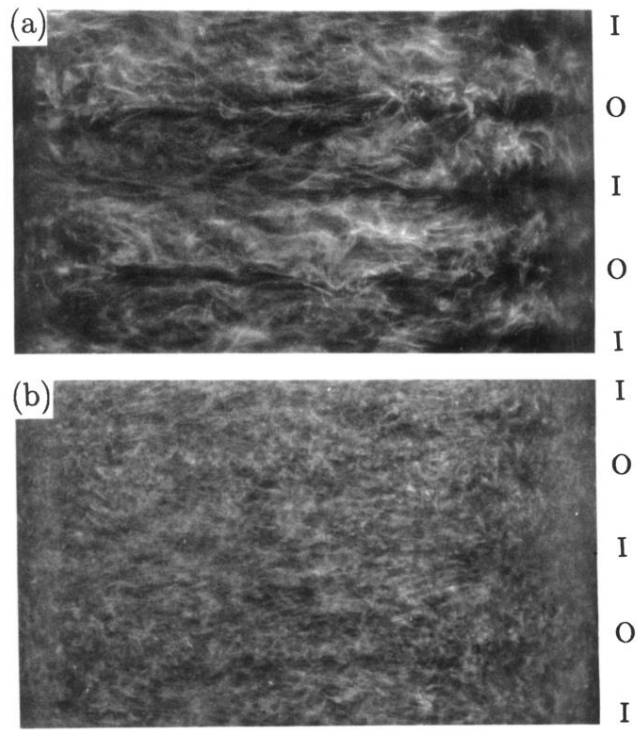


FIG. 1. Photographs of turbulent Taylor vortex flow at (a) $R = 4600$ and (b) $R = 15300$. (Taylor vortices first form at $R_c = 82.4$.) The four vortices shown are from an eight-vortex state, corresponding to an average axial wavelength of $2.87(b-a)$. The letters indicate the inflow (*I*) and outflow (*O*) boundaries.